ISSN 1027-4510, Journal of Surface Investigation. X-ray, Synchrotron and Neutron Techniques, 2015, Vol. 9, No. 3, pp. 576–580. © Pleiades Publishing, Ltd., 2015.
Original Russian Text © P.A. Ershov, S.M. Kuznetsov, I.I. Snigireva, V.A. Yunkin, A.Yu. Goikhman, A.A. Snigirev, 2015, published in Poverkhnost'. Rentgenovskie, Sinkhrotronnye i Neitronnye Issledovaniya, 2015, No. 6, pp. 55–59.

# High-Resolution X-ray Diffraction Based on 1D and 2D Refractive Lenses

**P. A. Ershov[a], S. M. Kuznetsov[b], I. I. Snigireva[c], V. A. Yunkin[b], A. Yu. Goikhman[a], and A. A. Snigirev[c]**

[a]*Kant Baltic Federal University, Kaliningrad, 236000 Russia*
[b]*Institute of Microelectronics Technology and High Purity Materials, Russian Academy of Sciences, Chernogolovka, Moscow oblast, 142432 Russia*
[c]*European Synchrotron Radiation Facility (ESRF), Grenoble, 38043 France*
*e-mail: fofan89@gmail.com*

Received September 10, 2014

**Abstract**—The results of studying a silicon–germanium (Si–Ge) nanoheterostructure using refractive X-ray optics are described. The diffraction patterns near the silicon Bragg-diffraction peak 400 in the focal plane of refractive lenses are recorded and analyzed. The experiments are carried out in two different geometries: using 1D and 2D X-ray compound refractive lenses.

*Keywords*: Si–Ge heterostructures, 1D and 2D X-ray refractive lenses, triple-crystal X-ray diffractometry

**DOI:** 10.1134/S1027451015030234

## INTRODUCTION

One of the fields of the development of nano- and microelectronics is the formation of small 3D semiconductor structures. An example of the application of these technologies is the detection of electromagnetic radiation by complementary metal-oxide-semiconductor (CMOS) matrices with several million pixels (semiconductor heterostructures) formed on a substrate [1]. The stable operation of these devices calls for optimization of the growth technology of semiconductor elements, which, in turn, requires accurate methods of monitoring and diagnosing the structural quality.

Nanoheterostructures are generally studied by triple-crystal X-ray diffractometry, which provides high-resolution reciprocal-space maps [2], on the basis of which one can draw conclusions about the structural quality of the nanoheterostructure. The development of third-generation synchrotrons allowed for the application of X-ray refractive optics along the entire optical path from undulators to detectors and X-ray cameras [3]. Refractive optics is traditionally used for focusing and collimating radiation; in addition, it can provide new techniques of X-ray diffraction and microscopy for synchrotron radiation sources [4, 5].

Previously, we proposed the use of X-ray refractive lenses as a Fourier analyzer, which made it possible to investigate 1D periodic silicon microstructures of different types under conditions of Bragg reflection [6]. In this study, we observe diffraction from the submicron 2D periodic grating of a Si–Ge heterostructure formed on a silicon substrate. To this end, we use 1D and 2D X-ray compound refractive lenses forming, respectively, a linear or point focal spot.

## EXPERIMENTAL

The experiments were performed on the ID06 station at the European Synchrotron Radiation Facility (ESRF). The optical elements included a transfocator [7] with 13 lenses (with a radius of curvature of 200 μm) and an assembly of 50 beryllium refractive lenses (with a radius of curvature of 50 μm). Images were recorded using a high-resolution Sensicam X-ray CCD camera with a pixel size of 0.645 μm and a field of 1376 × 1040 pixels.

The object of study was a Si–Ge nanoheterostructure [2], which represents germanium nanocrystals grown on the grating of silicon pillars with a period of 360 nm in the Si(110) crystal plane (Fig. 1). Pillars with a width of 90 nm and a length of 150 nm were formed on the Si(001) substrate according to the BiCMOS technology [8]. The structure was prepared at the IHP center (Frankfurt (Oder), Germany). The sample (a plate 20 × 20 mm in size) was studied using two different measurement geometries (Fig 2): *A* and *B*. Geometry *A* implied the use of the transfocator located closer to the source (see the table). This position of the focusing element makes it possible to reduce the angular aperture on the side of the image in the horizontal direction in comparison with unfocused radiation, which allows one to reduce the instrumental contribution to the crystal rocking curves. Focusing was per-

Experimental parameters

| Measurement scheme | X-ray energy, keV | Distance to the source $L$, m | Focal length $f$, cm | Distance from the sample to the camera $r$, cm |
|---|---|---|---|---|
| *A*. Transfocator before the sample, linear focusing | 24 | 39 | 1965 | 35 |
| *B*. 50 beryllium lenses before the sample, point focusing | 14 | 57 | 149 | 42 |

formed in the vertical direction. When measuring in geometry *B*, the assembly of 50 beryllium lenses was located closer to the sample. The radiation was focused in both the vertical and horizontal directions.

The Si(001) substrate plane was generally rotated by the angle θ and the camera was oriented so as to form the angle 2θ with the incident-radiation direction (Fig. 2). The angle θ corresponded to the Bragg-diffraction peak 400 from the Si sample surface. The X-ray camera recorded a series of images at different detuning angles Δθ from the angle θ.

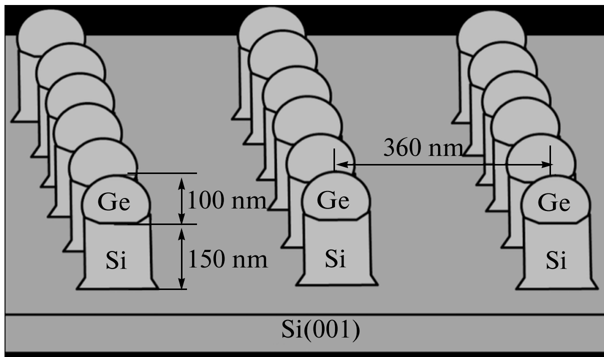


**Fig. 1.** Sketch of studied Si-Ge nanoheterostructure.

## MEASUREMENTS IN GEOMETRY *A*

In the case of focusing using the transfocator, we scanned the vicinity $\Delta q = \pm 8.30\ \mu m^{-1}$ of the Si Bragg-diffraction peak 400 with a step $\delta q = 0.83\ \mu m^{-1}$ (Fig. 3). To this end, cartridges with 12 refractive lenses with a radius of curvature of 200 μm and one refractive lens with a radius of curvature of 500 μm were mounted in the transfocator. No diffraction peaks (or nonzero Fourier components) caused by the submicron sample structure were found in this region. Nonzero Fourier components begin to arise upon crystal detuning by $\Delta q = 86\ \mu m^{-1}$ (Fig. 4). According to the relation between the observed-pattern period $T$ and the grating period $d$ [9],

$$d = \lambda r / T, \quad (1)$$

(λ is the wavelength and $r$ is the distance from the sample to the detector). The grating period $d$ is 341 ± 30 nm at the Fourier-component period $T = 55$ μm. The error in estimating the period is mainly related to the accuracy of determining the distances between the object and the camera.

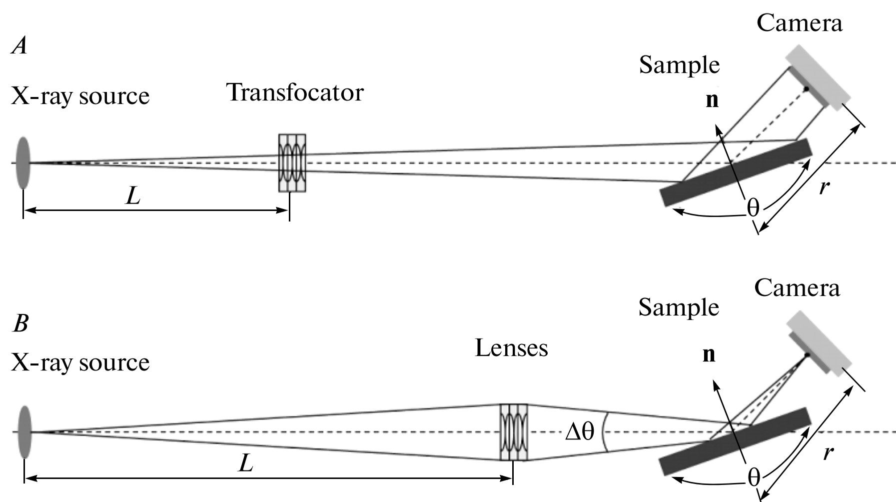


**Fig. 2.** Two schematics of the experiment: (*A*) linear focusing using the transfocator and (*B*) point focusing using an assembly of 50 beryllium lenses (top view).

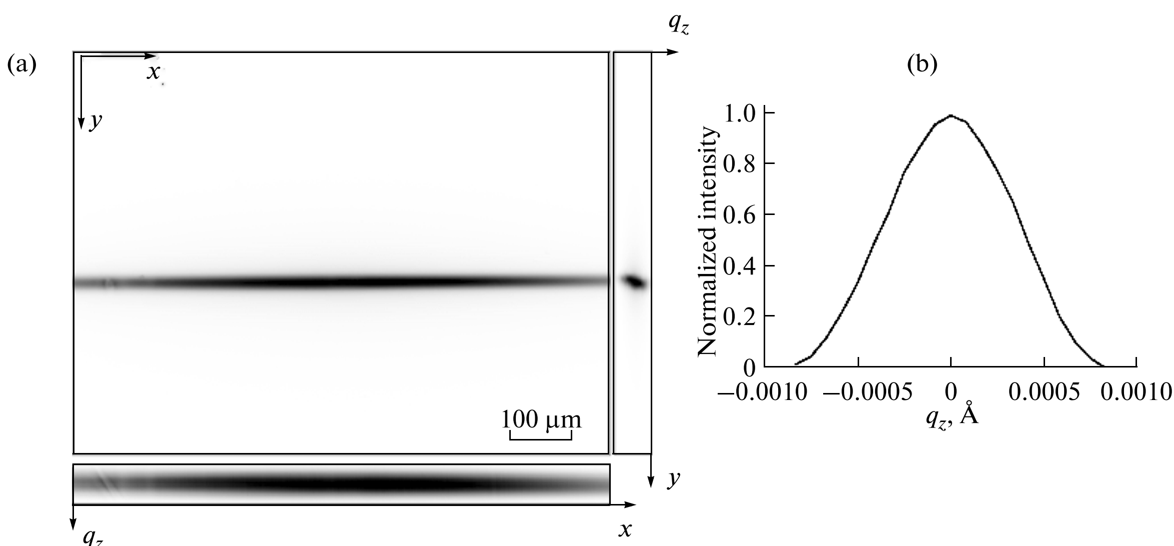


**Fig. 3.** (a) Image recorded by the CCD camera and orthogonal projections when the crystal is rotated; (b) analyzed rocking curve of the Si Bragg-diffraction peak 400 (geometry $A$).

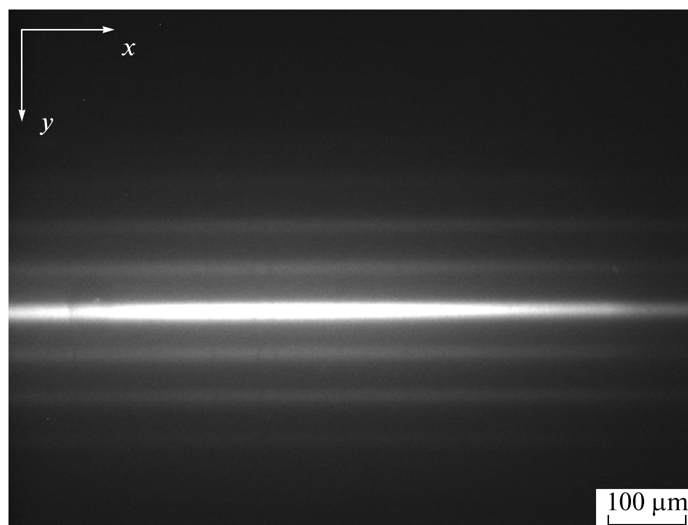


**Fig. 4.** X-ray diffraction pattern formed upon crystal detuning from the Si Bragg-diffraction peak 400 by $\Delta q_z = -0.0086$ Å$^{-1}$. The Fourier-component period is $T = 55$ μm.

The image obtained by the camera also contains pattern distortions related to the presence of defects in the sample, which yield contrast at the observed Fourier components. Hence, use of the transfocator makes it possible to do the Fourier transform in one direction and obtain a topographic image of the analyzed region, limited by the projection of the source, in the other direction.

## MEASUREMENTS IN GEOMETRY $B$

In the case of focusing using 50 beryllium lenses, we scanned the vicinity $\Delta q = \pm 15$ μm$^{-1}$ of the Si Bragg-diffraction peak 400 with a step of $\delta q = 1$ μm$^{-1}$ (Fig. 5). In contrast to the case $A$, the Fourier components are observed under exact Bragg conditions for the silicon diffraction peak 400. The reason is that the X-ray beam in the case $B$ is also focused in the diffraction plane, which allows one to observe the diffraction pattern in the range of angles of radiation incidence. The angular range $\delta\theta$ (Fig. 2) for $B$ is determined by the effective aperture $A_{\text{eff}}$ and the focal length of the lens $f$:

$$\delta\theta = A_{\text{eff}}/f. \quad (2)$$

In case $B$, 50 beryllium lenses with a radius of curvature of 50 μm at a X-ray energy of $E$ = 14 keV ($A_{\text{eff}} = 645$ μm) and focal length of 149 cm yield the angular range $\delta\theta = 0.0248$ deg, which corresponds to

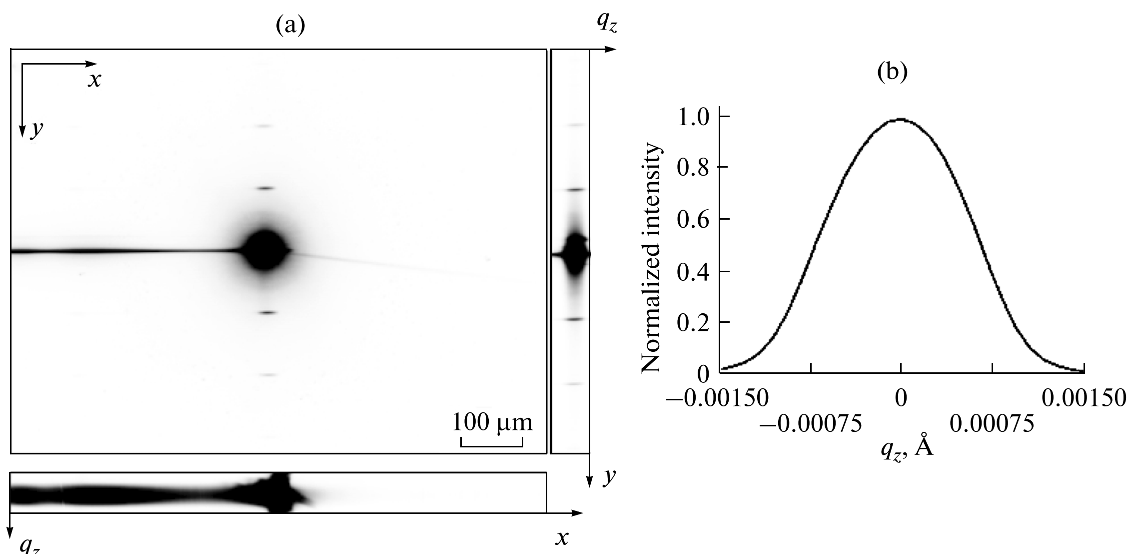


**Fig. 5.** (a) X-ray diffraction pattern recorded by the CCD camera and orthogonal projections when the crystal is rotated; (b) analyzed rocking curve of Si Bragg-diffraction peak 400 (geometry *B*).

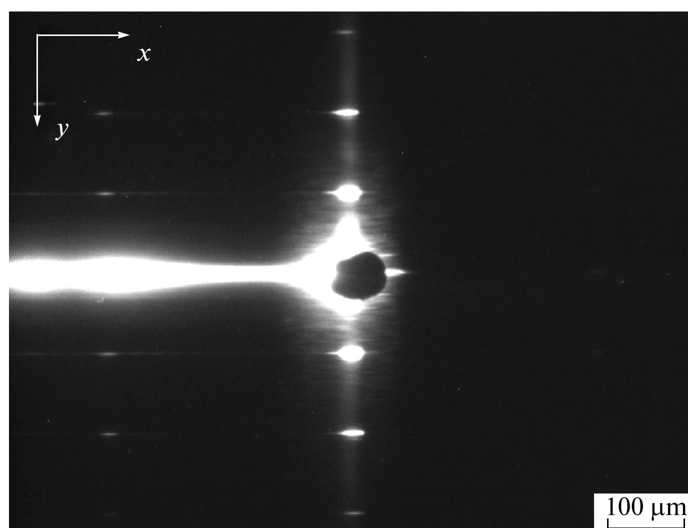


**Fig. 6.** Measurements in geometry *B*: image recorded by the CCD camera under the exact Bragg condition for the Si Bragg-diffraction peak 400 using the beam stop.

$\Delta q = 62\ \mu m^{-1}$ in terms of the reciprocal-space vector. Thus, the pattern observed at the detector is a superposition of patterns formed under different conditions of X-ray beam incidence on the sample. In this case, a strong line shifts in the diffraction plane from the zero Fourier component to small angles θ of X-ray beam incidence. This line indicates reflections from deformed silicon pillars with a lattice parameter larger than that of the silicon substrate, which is confirmed by the published data of triple-crystal X-ray diffraction from a similar sample [2].

When using a beam stop, which is an X-ray-opaque cylinder 72 μm in diameter placed directly before the detector using a thin wire 13 μm in diameter, we found Fourier components forming a 2D periodic pattern (Fig. 6). The pattern's period along the *y* direction was $T_y = 104 \pm 2$ μm, which corresponds to the grating period $d = 358 \pm 30$ nm according to formula (1). The period along the *x* direction differs from that along the *y* direction. Since the sample is rotated by the angle $\theta = 19.16$ deg, the observed pattern is distorted along the *x* direction and is a projection on the X-ray beam-inci-

dence plane. The period $T_x$ is recalculated according to the expression

$$T_x = T_x' \sin\theta, \quad (3)$$

where $T_x'$ is the observed period along the $x$ direction. Then, if $T_x' = 314$ μm, $T_x = 103 \pm 2$ μm, which corresponds to the period $T_y$. The data obtained completely correlate with the nominal values within measurement error.

Along with Fourier components, Fig. 6 also contains artifacts related to specific features of the experimental geometry. First, the long line passing along the $y$ direction through the image center corresponds to diffraction from a rectangular slit used to collimate the radiation before the lens. Second, a component related to small-angle scattering from the material of the beryllium lenses (grain halo near the beam stop) is also presented in the image.

## CONCLUSIONS

We demonstrated the possibility of using refractive lenses as a tool of high-resolution X-ray diffraction. The vicinity of the silicon Bragg-diffraction peak 400 was investigated for a Si–Ge nanoheterostructure forming a 2D periodic grating in the (110) plane. The diffraction angles for this structure were on the order of several hundred microradians at an angular resolution of the assembled experimental schemes of ~10 μrad.

Two types of focusing (2D and 1D) were used. 1D focusing made it possible to obtain a topographic image of the analyzed region in the diffraction plane and the Fourier transform of the analyzed structure in the perpendicular direction. This geometry of the experiment is convenient for searching for defect-free portions on the sample and simultaneous Fourier transform of the analyzed regions. In the case of 2D focusing, the diffraction orders were resolved in two directions. Due to radiation focusing in the diffraction plane, the superposition of images was observed on the camera screen for the range of angles of incidence Δθ. This geometry of the experiment is convenient for adjustment of the spatial orientation of the nanostructure because two directions can be analyzed simultaneously. It can also be used for the formation of crystal rocking curves without sample rotation, which is convenient for studying the grating dynamics.

Advantages of the used technique are as follows: flexibility of the experimental scheme due to the use of transfocators; convenience of adjustment and measurements in comparison with the use of crystals; the possibility of reducing the duration of the experiments; high angular resolution; and the possibility of observing reflection from a crystal in a certain range of angles of incidence.

## ACKNOWLEDGMENTS

We are grateful to Dr. P. Zaumseil for supplying us with samples of te Si–Ge nanoheterostructure, as well as Dr. C. Detlefs, P. Wattecamps, and M. Lyubomirskii for help in carrying out the experiments on the ID06 station at the European Synchrotron Radiation Facility (ESRF).

This study was supported by the Ministry of Education and Science of the Russian Federation, project nos. 14.Y26.31.0002 and 02.G25.31.0086.

## REFERENCES

1. N. Wermes, Nucl. Instrum. Methods Phys. Res. A **512**, 277 (2003).
2. P. Zaumseil, Y. Yamamoto, A. Bauer, et al., J. Appl. Phys. **109**, 023511 (2011).
3. A. Snigirev, V. Kohn, I. Snigireva, and B. Lengeler, Nature **384**, 49 (1996).
4. M. Drakopoulos, A. Snigirev, I. Snigireva, and J. Schilling, Appl. Phys. Lett. **86**, 014102 (2005).
5. A. Petukhov, J. Thijssen, and D. J. Hart, J. Appl. Crystallogr. **39**, 137 (2006).
6. P. Ershov, S. Kuznetsov, I. Snigireva, et al., J. Appl. Crystallogr. **46**, 1475 (2013).
7. A. Snigirev, I. Snigireva, G. Vaughan, et al., J. Phys.: Conf. Ser. **186**, 012073 (2009).
8. H. Rücker, B. Heinemann, W. Winkler, et al., in *Proceedings of IEEE Bipolar/BiCMOS Circuits and Technology Meeting BCTM, Oct. 12–14, 2009* (IEEE, 2009), p. 166.
9. J. Goodman, *Introduction to Fourier Optics*, 3rd ed. (Roberts and Company, Englewood, 2005).

*Translated by A. Sin'kov*